

See discussions, stats, and author profiles for this publication at: <https://www.researchgate.net/publication/51405667>

# Response of Nanoparticle-Based One-Dimensional Photonic Crystals to Ambient Vapor Pressure

ARTICLE *in* LANGMUIR · AUGUST 2008

Impact Factor: 4.46 · DOI: 10.1021/la801210q · Source: PubMed

---

CITATIONS

70

---

READS

67

## 4 AUTHORS, INCLUDING:



[Agustin R. Gonzalez-Elipse](#)

Spanish National Research Council

**434** PUBLICATIONS **7,332** CITATIONS

SEE PROFILE



[Hernán Míguez](#)

Spanish National Research Council

**164** PUBLICATIONS **5,356** CITATIONS

SEE PROFILE

# Response of Nanoparticle-Based One-Dimensional Photonic Crystals to Ambient Vapor Pressure

S. Colodrero, M. Ocaña, A. R. González-Elipe, and H. Míguez\*

*Instituto de Ciencia de Materiales de Sevilla, Consejo Superior de Investigaciones Científicas (CSIC),  
Américo Vespucio 49, 41092 Sevilla, Spain*

*Received April 17, 2008. Revised Manuscript Received May 23, 2008*

Herein we report an analysis of the variation of the optical properties of different nanoparticle-based one-dimensional photonic crystal architectures versus changes in the ambient vapor pressure. Gradual shift of the optical response provides us with information on the sorption properties of these structures and allow us to measure precise adsorption isotherms of these porous multilayers. The potential of nanoparticle-based one-dimensional photonic crystals as base materials for optical sensing devices is demonstrated in this way.

## I. Introduction

The advent of porous photonic crystals has generated a great deal of interest in the field of sensing because of the possibility that they offer to monitor compound separation and recognition through the change in the optical response caused by the presence of targeted species.<sup>1</sup> Different variations of the same concept have been demonstrated in the past years showing its great potential.<sup>2–6</sup> Conversely, the controlled change of the optical response by means of an external agent has been used to develop color displays that can cover the whole visible spectrum.<sup>7</sup> Many of these achievements have mainly been possible because of the existence of an accessible porous network in three-dimensionally ordered packings of monodisperse, submicrometer-size colloids<sup>8,9</sup> or their replicas.<sup>10</sup> Be it by direct infiltration of the targeted compounds within the voids<sup>11</sup> or by previous infiltration of a material that can capture them,<sup>12,13</sup> the principle behind the controlled optical response of such materials is always the same: The presence of a guest compound within the lattice gives rise to a change in either the dielectric constant of the pores or in the lattice constant of the crystal, which affects the intensity, spectral position, and width of the bright colored Bragg reflections these structures display. Some two-dimensional photonic crystals also present an ordered porosity that can be accessed from outside, allowing for control of the optical response through ambient conditions.<sup>5,6</sup> Interestingly, there are no examples of one-dimensional photonic crystal films that present similar properties,

although these structures are usually easier to build than those of higher dimensionality and present very intense and wide Bragg reflections, which make them excellent candidates as constituents of devices. However, for most optical applications, multilayers made of dense phases have so far been preferred to porous ones.<sup>14</sup>

Very recently, new types of one-dimensional photonic crystals with controlled porosity have been prepared by alternate deposition of either mesoporous<sup>15,16</sup> or nanoparticle-based<sup>17,18</sup> films. The advantage of such lattices lies on the wide range of materials available to be deposited as multilayers, which implies accurate control over the optical properties of the periodic ensemble, on the high structural and optical quality attainable, and on their ease of functionalization and integration in devices.<sup>19</sup> The environmental response of such lattices has already been tested through the infiltration of different types of liquids.<sup>15,16,18</sup> Also, an important feature of porous photonic crystals is their capability to gradually respond to small changes of the ambient gas pressure. This behavior has been observed for both three-<sup>20</sup> and one-dimensional photonic crystals.<sup>21</sup> In this latter case, a complex response versus varying gas pressure was reported for multilayers made of films in which an ordered mesoporosity had been built up. This was attributed to the interplay between the gas adsorption and condensation processes taking place in neighboring layers in the stack.

Here, different types of nanoparticle-based photonic crystal architectures are used to study their sorption properties versus various solvent vapors. These structures are obtained through the alternate deposition of layers of nanoparticles of different composition by spin-coating as described in ref 18. SiO<sub>2</sub> and TiO<sub>2</sub> are the materials employed in the production of this multilayer stack due to the high refractive index contrast between them, which allow us to attain well-defined Bragg reflection

\* Author to whom correspondence and request of materials should be addressed. E-mail: hernan@icmse.csic.es.

- (1) Alivisatos, P. *Nat. Biotechnol.* **2004**, *22*, 47.
- (2) Holtz, J. H.; Asher, S. A. *Nature* **1997**, *389*, 829.
- (3) Blanford, C. F.; Schrodin, R. C.; Al-Daous, M.; Stein, A. *Adv. Mater.* **2001**, *13*, 26.
- (4) Lee, Y. J.; Braun, P. V. *Adv. Mater.* **2003**, *15*, 563.
- (5) Li, Y. Y.; Cunin, F.; Link, J. R.; Gao, T.; Betts, R. E.; Reiver, S. H.; Chin, V.; Bhatia, S. N.; Sailor, M. J. *Science* **2003**, *299*, 2045.
- (6) Chow, E.; Grot, A.; Mirkarimi, L. W.; Sigalas, M.; Girolami, G. *Opt. Lett.* **2004**, *29*, 1093.
- (7) Arsenault, A. C.; Puzzo, D. P.; Manners, I.; Ozin, G. A. *Nat. Photonics* **2007**, *1*, 468.
- (8) Jiang, P.; Bertone, J. F.; Hwang, K. S.; Colvin, V. L. *Chem. Mater.* **1999**, *11*, 2132.
- (9) Míguez, H.; López, C.; Meseguer, F.; Blanco, A.; Vázquez, L.; Mayoral, R.; Ocaña, M.; Fornés, V.; Mifsud, A. *Appl. Phys. Lett.* **1997**, *71*, 1148.
- (10) Stein, A. *Microporous Mesoporous Mater.* **2001**, *44*, 227.
- (11) Kamp, U.; Kitaev, V.; von Freymann, G.; Ozin, G. A.; Mabury, S. A. *Adv. Mater.* **2005**, *17*, 438.
- (12) Lee, K.; Asher, S. A. *J. Am. Chem. Soc.* **2000**, *122*, 9534.
- (13) Arsenault, A. C.; Míguez, H.; Kitaev, V.; Ozin, G. A.; Manners, I. *Adv. Mater.* **2003**, *15*, 503.

(14) Macleod, H. A. *Thin Film Optical Filters*, 3rd ed.; Institute of Physics Publishing: London, 2001 (ISBN 0750306882).

(15) Choi, S. Y.; Mamak, M.; von Freymann, G.; Chopra, N.; Ozin, G. A. *Nano Lett.* **2006**, *6*, 2456.

(16) Fuertes, M. C.; López-Alcaraz, F. J.; Marchi, M. C.; Troiani, H. E.; Míguez, H.; Soler Illia, G. J. A. *Adv. Funct. Mater.* **2007**, *17*, 1247.

(17) Wu, Z.; Lee, D.; Rubner, M. F.; Cohen, R. E. *Small* **2007**, *3*, 1445.

(18) Colodrero, S.; Ocaña, M.; Míguez, H. *Langmuir* **2008**, *24*, 4430.

(19) Calvo, M. E.; Colodrero, S.; Rojas, C. T.; Ocaña, M.; Anta, J. A.; Míguez, H. *Adv. Funct. Mater.* **2008**, in press.

(20) Arsenault, A. C.; Kitaev, V.; Manners, I.; Ozin, G. A.; Mihi, A.; Míguez, H. *J. Mater. Chem.* **2005**, *15*, 133.

(21) Fuertes, M. C.; Colodrero, S.; Lozano, G.; Gonzalez-Elipe, A. R.; Grosso, D.; Boissiere, C.; Sanchez, C.; Soler-Illia, G. J. A. A.; Míguez, H. *J. Phys. Chem. C* **2008**, *112*, 3157.

peaks with only a few layers in the stack. We demonstrate that nanoparticle-based photonic crystals are very easily accessed from outside as we get nonordered mesopores inside the  $\text{SiO}_2/\text{TiO}_2$  Bragg reflector with a very high connectivity. In situ analysis of the changes of the optical properties is performed for both purely periodic and controlled defect containing lattices, with optical adsorption isotherms being attained for both of them. The potential of nanoparticle-based one-dimensional photonic crystals as base materials for optical sensing devices is demonstrated in this way.

## II. Nanoparticle-Based 1D Photonic Crystal Preparation

Several samples were prepared by using  $\text{SiO}_2$  and  $\text{TiO}_2$  nanoparticles with different size distributions centered around 5 and 15 nm, respectively.  $\text{TiO}_2$  crystallites were synthesized using a procedure based on the hydrolysis of titanium isopropoxide (97%, Aldrich), followed by growth under hydrothermal conditions.<sup>22</sup>  $\text{SiO}_2$  colloids were purchased from Dupont (LUDOX TMA, Aldrich). Precursor suspensions for the spin-coating process were prepared employing 79%:21 vol % vol. mixtures of  $\text{MeOH}/\text{H}_2\text{O}$ . Drops of these suspensions were alternatively spread onto a previously treated square glass substrate and spun at constant velocity using an SCI series Novocontrol GmbH Spin Coater operating at atmospheric pressure. Each film thickness can be tuned between 40 and 200 nm by changing the rotation speed of the substrate or the concentration of the suspensions. No intermediate stabilization processes are necessary to obtain high optical quality films. A final heating of the multilayer at 450 °C in a furnace provides the structure with the mechanical stability required for all ulterior processes without generating cracks or any deterioration of the optical quality. Both an eight-layer Bragg stack and a 13-layer Bragg stack containing a silica nanoparticle defect built in the middle are studied in this paper. The former is made of 5 wt % precursor solutions of  $\text{SiO}_2$  and  $\text{TiO}_2$  particles. The latter is made of silica (3 wt %) and titania (5 wt %), and the  $\text{SiO}_2$  nanoparticle defect is about 3 times as thick as those layers forming the periodic structure. The rotation speed is set at 100 rps in all cases.

Field emission scanning electron microscopy (FESEM, Hitachi 5200 operating at 5 kV) images corresponding to the above-mentioned nanoparticle-based one-dimensional photonic crystals are shown in Figure 1. The uniformity of the thickness of both types of layers over long distances can be observed, which ensures the good optical quality of the ensemble. Figure 1a,c shows low-magnification images of a cross section of the eight-layered Bragg reflector and of the periodic structure in which a  $\text{SiO}_2$  defect layer has been built, respectively. A magnified view of the different size and morphology of nanoparticles used is presented in Figure 1b. A slight penetration of the smaller (in average)  $\text{TiO}_2$  particles occurs when they are deposited onto an already formed layer of larger  $\text{SiO}_2$  colloids. As shown below, this does not significantly affect the fact that we can achieve a high dielectric contrast between neighboring layers. On the other side, it can be clearly seen in Figure 1b that, when  $\text{SiO}_2$  colloids are deposited onto a  $\text{TiO}_2$  nanoparticle layer, the latter behaves as an impenetrable slab.

## III. Optical Response versus Varying Ambient Pressure: Experiment and Discussion

It is well-known that multilayered structures present brilliant colored reflections when their photonic band gaps fall into the visible region of the spectrum. These periodic stacks with alternate regions of high and low refractive index cause constructive interference of the coherently scattered beams for a certain range of incident frequencies in the backward direction, yielding an intense reflectance peak. As shown in Figure 1, we

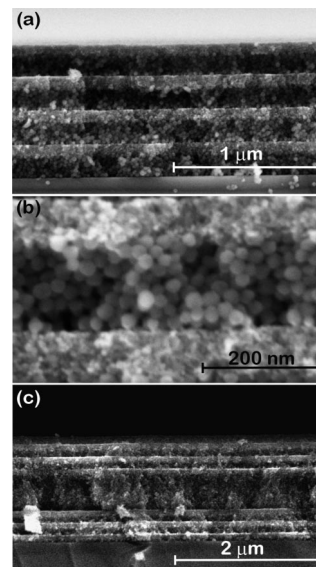


**Figure 1.** Structural characterization of nanoparticle-based one-dimensional photonic crystals. (a) FESEM image of a cross section of an eight-layered Bragg reflector made of silica and titania nanocolloids, and (b) magnified view of the spherical particles ( $\text{SiO}_2$ ) and the smaller crystallites ( $\text{TiO}_2$ ) composing the 1D photonic crystal. The lattice parameter of the periodic structure built in both cases is  $220 \pm 10$  nm. (c) FESEM image showing a silica defect layer built in the center of the stack. It can be clearly seen that the thickness of this layer is about 5 times thicker than those forming the multilayer structure. The optical cavity is sandwiched between three-layer  $\text{TiO}_2$ – $\text{SiO}_2$  photonic crystals. In this case, the lattice parameter is  $170 \pm 10$  nm.

can controllably modify the thickness of the deposited layers in the stack and therefore the spectral position of the reflectance maximum.<sup>18</sup> On the other hand, the intensity and width of such Bragg reflections depend mainly on the contrast between the refractive index of the different types of layers. Both features are very sensitive to the presence of guest species in the void space between nanoparticles because of the variation of the average refractive index of each layer they give rise to. In order to analyze the change of the optical response with the vapor pressure in the environment, we measure the specular reflectance spectra for the aforementioned structures at different partial pressures of isopropanol and water vapors.

The variation of the optical response with the vapor pressure was measured using a Bruker IFS-66 FTIR spectrophotometer attached to a microscope with a  $4\times$  objective with 0.1 of numerical aperture (light cone angle  $\pm 5.7^\circ$ ). In order to do so, the multilayers structures were introduced in a closed chamber in which the partial pressure of a volatile liquid could be varied from  $P/P_0 = 0$  up to  $P/P_0 = 1$  ( $P_0$  being the saturation vapor pressure of the liquid at room temperature). The chamber possesses a flat quartz window through which the reflectance spectra at normal incidence were measured in situ. In Figure 2a, we plot the evolution of the optical response observed for the eight-layered Bragg stack as the partial pressure of isopropanol vapor (refractive index  $n = 1.377$ ) was varied. The observed changes in the reflectance peak spectral position (blue circles) and intensity (red triangles) are plotted in Figure 2b. From the increase in the peak intensity observed at low  $P/P_0$ , we can conclude that the dielectric contrast between adjacent layers is increased, which indicates that solvent adsorption occurs gradually and preferentially within micropores present in the high refractive index layer (in our case,  $\text{TiO}_2$ ). Contrarily, at  $P/P_0 \approx 0.7$ , an abrupt decrease in the intensity of the reflection maximum is detected, indicating a rapid decrease of the dielectric contrast between the

(22) Burnside, S. D.; Shklover, V.; Barbé, C.; Comte, P.; Arendse, F.; Brooks, K.; Grätzel, M. *Chem. Mater.* **1998**, *10*, 2419.

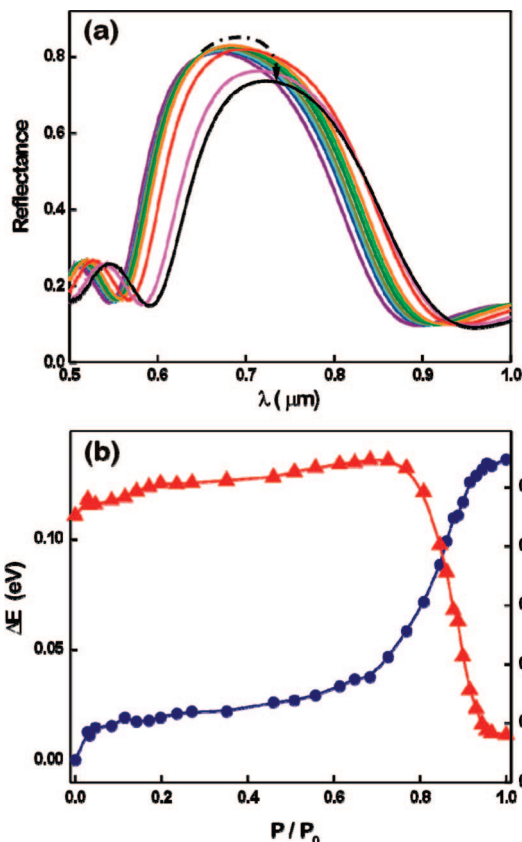


**Figure 2.** (a) Specular reflectance spectra corresponding to the eight-layered Bragg reflector at different partial pressures of isopropanol vapor. The increase in the isopropanol vapor partial pressure from 0 to 1 is indicated by the arrow. (b) Evolution of both the maximum spectral position (blue circles) and its intensity (red triangles) for this periodic stack at different partial pressures of vapor.

two types of layers, which should be caused by condensation within the pores of the silica layer. The evolution of the spectral position of the reflectance maxima as the partial pressure of isopropanol vapor increases is in good agreement with the behavior inferred from the evolution of the peak intensity. An energy scale is used to plot the peak shift, so the observed change is independent of the spectral range in which it takes place. For low  $P/P_0$ , the shift of the Bragg peak toward higher wavelengths implies an increase of the average refractive index of the multilayer stack as a consequence of the gradual adsorption of vapor onto the nanoparticle walls. For  $P/P_0 \approx 0.7$ , the abrupt red-shift observed indicates rapid condensation within the mesopores of the structure, as was concluded from the analysis of the variation of the peak intensity. It should be noted that the peak shift by itself gives no information on the preferential adsorption or condensation in a specific type of layer. Such details can only be extracted from the analysis of the dependence of peak intensity with  $P/P_0$ . However, rapid changes of the intensity (dielectric contrast) should be accompanied by similar changes of the peak spectral position (average dielectric constant).

Figure 3a displays the whole series of spectra obtained for an eight-layered structure as the partial pressure of water (refractive index  $n = 1.333$ ) is gradually increased in the chamber. This lattice is the same as that whose response versus isopropanol vapor pressure was shown in Figure 2. A rather different behavior is found when compared to Figure 2a. As in the previous case, the evolution of both the maximum spectral position (blue circles) and its intensity (red triangles) at different partial pressures of water vapor are plotted in Figure 3b. Noteworthy, the total shift

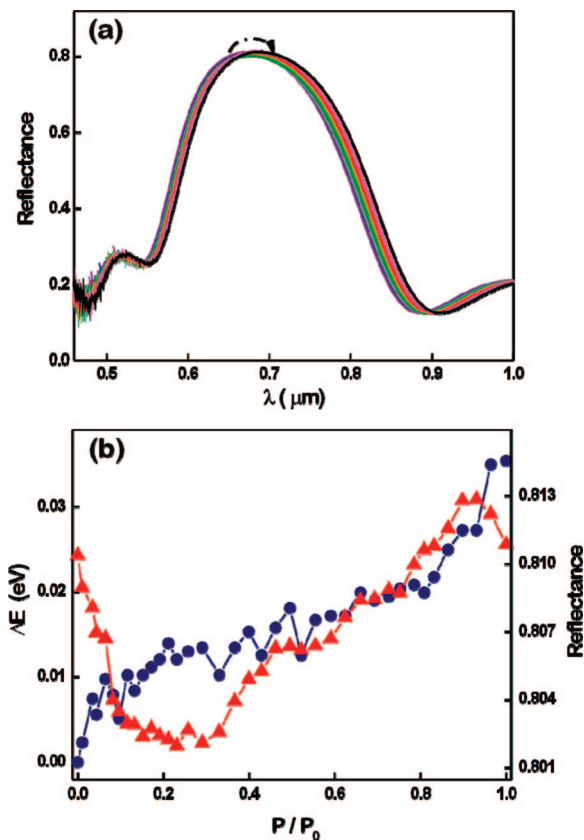


**Figure 3.** (a) Optical response of the multilayer structure with eight alternated layers at different partial pressures of water vapor. The increase in the water vapor partial pressure from 0 to 1 is indicated by the arrow. (b) Evolution of both the maximum spectral position (blue circles) and its intensity (red triangles) at different partial pressures of vapor.

of the reflectance spectra to longer wavelengths is much smaller in this case than in the case of the adsorption of isopropanol vapor. The spectral position of the Bragg peak changes 0.14 eV as a result of isopropanol condensation within the pores, whereas it changes only by 0.035 eV when exposed to water vapor. This dissimilar response cannot be attributed to the small refractive index difference between both compounds, but to the different affinity of the pore walls for the different adsorbed species. It shows that the adsorption properties of nanoparticle-based multilayers strongly depend on the type of compound vaporized in the chamber and constitutes a proof of concept of the interest of these multilayers in sensing devices. Correspondingly, peak intensity shows tiny variations, further confirming the absence of significant adsorption of the ambient water within the pores. A decrease of less than 1% intensity is observed at  $P/P_0 < 0.1$  followed by a gradual recovery of the initial intensity for  $P/P_0 > 0.2$ . These results indicate that the nanoparticle-based multilayers might present a rather hydrophobic character, in good agreement with other recent analyses about mesoporous  $\text{SiO}_2/\text{TiO}_2$  stacks.<sup>17,16</sup>

Detailed information on the variation of the refractive index of each layer in the stack as the vapor pressure in the chamber changes can be extracted from the analysis of the optical reflectance spectra. These were fitted using a model based on the scalar wave approximation,<sup>23,16,18</sup> in which the thickness of each film can vary up to 10% around the input initial values measured in FESEM images in order to account for experimental errors. The refractive indexes of both types of layers are left as adjustable



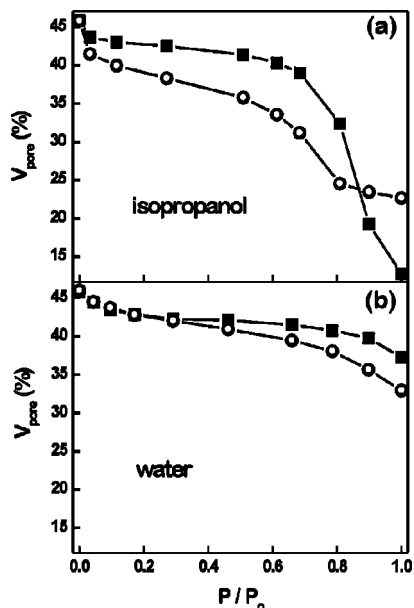


**Figure 4.** (a,b) Evolution of the free pore volume (%) for the titania (open circles) and silica (closed squares) layers at different partial pressures of isopropanol and water vapors, respectively. A Bruggeman expression for a three-component system has been used in order to estimate such values.

variables. The model assumes that all layers with equal composition and porosity in the stack will present the same refractive index in equilibrium conditions with a given vapor pressure. The optimum fit is chosen by comparison with the experimental spectrum using the method of squared minima. By doing so, we estimate the variation of the refractive index as vapor pressure increases for each layer independently and, therefore, the evolution of the free pore volume fraction. In order to do so, we use the Bruggeman expression<sup>24</sup> for a three-component dielectric medium (oxide–liquid–air). This thorough analysis allows a quantification of the phenomena previously pointed out as the origin of the observed optical response and a detailed description of them. Figure 4 shows the evolution of the free pore volume (%) both for the titania (open circles) and for the silica (closed squares) layers at different partial pressures of isopropanol and water vapor. In these graphs we have used the same scale in order to compare the adsorbed volume on each layer with the different solvents. Some interesting features arise from this analysis. Isopropanol adsorb preferentially and gradually onto the TiO<sub>2</sub> pore walls at lower partial pressures and condense abruptly within the pores of both the SiO<sub>2</sub> and TiO<sub>2</sub> layers simultaneously at  $P/P_0 \approx 0.7$ . On the other side, water vapor adsorption, although much more inefficient, also takes place simultaneously within TiO<sub>2</sub> and SiO<sub>2</sub> pores for  $P/P_0 > 0.4$ . This concurrent condensation in pores of very different size suggests that the solvent adsorption–condensation behavior in one kind of layer could be influenced by the porosity characteristics of an adjacent porous layer. It reveals that the response to the chamber pressure of the larger pore layer is mediated, and to some extent determined, by the smaller pore layer, which in our case is the TiO<sub>2</sub> nanoparticle layer. Once condensation within the smaller pores occurs, the vapor pressure at which the larger pore layer is subjected to is no longer determined by the vapor pressure measured in the chamber. This observation is in good agreement with the conclusions extracted from similar previous

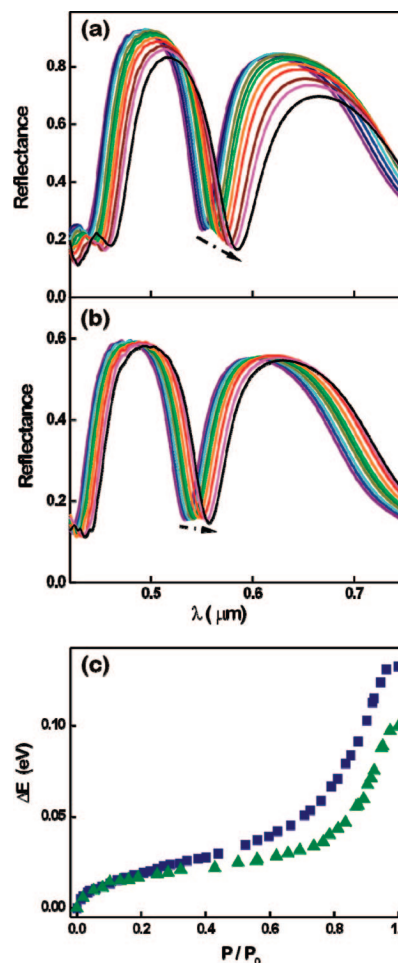


**Figure 5.** (a,b) Optical response of the multilayer structure with a planar defect after being exposed to different partial pressures of isopropanol and water vapors, respectively. The arrow indicates the increase in the vapor partial pressure from 0 to 1. (c) Evolution of the position of the reflectance dip corresponding to the defect state within the bandgap for different partial pressures of isopropanol (blue squares) and water (green triangles).

analysis of different porous periodic multilayers.<sup>21</sup> Additionally, these results confirm that optical reflectance is a powerful tool to attain information on the sorption properties of complex structures made by stacking films of different porosity and composition. In this regard, it is worth noting that methods so far reported to analyze the porosity of microporous and mesoporous materials are difficult to apply to thin films successfully, with the exception of ellipsoporosimetry. With this latter technique, however, because of the complexity of the data analysis, the maximum number of layers that has been analyzed is two, as it has been previously reported.<sup>21</sup> The main limiting factor when applying other techniques developed for pore size determination is the amount of sample present in films, which in our case is lower than 0.01 g, so no reliable results can be expected. Scratching several samples to reach the required minimum weight is an option that presents serious drawbacks, since pieces of the substrate are usually mixed with the mesoporous film, hence yielding large errors in the sample weight and incorrect results, as has been pointed out before.<sup>25</sup>

Also, the optical response of a one-dimensional photonic crystal structure containing a SiO<sub>2</sub> nanoparticle defect built in at different partial pressures of isopropanol and water vapors was studied,

(24) van de Hulst, H. C. *Light Scattering by Small Particles*; Dover Publications: New York, 1981 (ISBN 0486642283).

(25) Nossov, A.; Haddad, E.; Guenneau, F.; Mignon, C.; Gédéon, A.; Grosso, D.; Babonneau, F.; Bonhomme, C.; Sanchez, C. *Chem. Commun.* **2003**, 2476.

and results are presented in Figure 5. Disruption of the periodicity, achieved by depositing a layer of different thickness in the middle of the stack, is expected to lead to localized photon states in the gap. Sharp dips within the reflectance peak corresponding to the forbidden band gap frequency range are the fingerprints of these states and provide us with a tool to monitor more precisely the peak shifts induced by vapor adsorption. The variation of the position of the reflectance dip for different partial pressures of isopropanol and water vapor is displayed in Figure 5c. Very well-defined optical adsorption isotherms are attained for defect-containing multilayers, as a result of the higher resolution provided by the thinner reflectance dip caused by the defect layer. Again in this case, the effect of the different affinity of the multilayer for water and isopropanol vapors is readily seen.

#### IV. Conclusions

We have demonstrated that the optical response of porous nanoparticle based one-dimensional photonic crystals is sensitive to environmental vapor pressure variations. The magnitude of the changes observed depend strongly on the type of compound adsorbed, which serves as a proof of concept of the capability these materials offer to perform selective detection of species. In good agreement with previous observations reported for other periodic multilayers, we find that sorption properties of the stack are determined by the interaction between neighboring layers. Different photonic crystal architectures are studied to prove the generality of the proposed concept.

LA801210Q